

Received November 16, 2020; reviewed; accepted January 11, 2021

Separation of fine beryl from quartz via magnetic carriers by the aiding of non-ionic surfactant

Mona M. Fawzy

Nuclear Materials Authority, Cairo, Egypt

Corresponding author: mm1_fawzy@yahoo.com

Abstract: This study demonstrated the possibility of separating fine beryl from quartz by using magnetic carrier technology with the presence of non-ionic surfactant (Sorbitan monooleate). Oleate-coated magnetite was used as a magnetic carrier for enhancing the magnetic properties of fine beryl to be separated and get rid of the most common associated gangue mineral "quartz". This study proved that the most important factors affecting this separation process is the pH, as the study showed that the efficiency of the separation process is the maximum possible when pH at the isoelectric point (IEP) of beryl. Where at IEP, beryl is ready to adsorb oleate-coated magnetite onto its surface and the presence of sorbitan monooleate helps this adsorption and strengthens. To demonstrate the separation process, physico-chemical surface characterization for beryl, quartz, magnetite and oleate-coated magnetite was studied before and after treatment with sorbitan monooleate using zeta potential measurements and Fourier Transform Infrared (FTIR). Mineralogical characterization was take place for separated minerals of beryl, quartz and magnetite using x-ray diffraction (XRD) analyses and scanning electron microscope (SEM) with energy-dispersive spectrometer (EDS) unit. The magnetic carrier separation tests were performed in this study in the case of separate minerals investigated that fine beryl (94% recovery) could be recovered under optimum test conditions of 2.5 pH, 4.29 g/L sorbitan monooleate and 1:0.5 beryl to oleate-coated magnetite ratio, while quartz under the same conditions was recovered by 9.8%. FTIR measurements for the investigated minerals before and after treatment with sorbitan monooleate confirmed that the adsorption of sorbitan monooleate on the surface of beryl far exceeds that of the surface of quartz at beryl IEP.

Keywords: beryl, magnetic carrier, sorbitan monooleate, oleate-coated magnetite, zeta potential, FTIR

1. Introduction

Beryl and bertrandite are the main ore sources of beryllium all over the world. The famous beryl deposits (emerald variety) of Egypt were known since ancient times in the southern part of the Eastern Desert of Egypt. As a result of these ancient mining processes, now Egypt is endowed with a unique source of beryl that is occurred as huge tailing dumps rich in non-gem crystals of fine beryl (Harrell, 2004, 2006). The most common associated gangue minerals with beryl are quartz, feldspar and mica. Because quartz is the most abundant and has similar physical properties to beryl (almost have the same specific gravity, magnetic and electric properties) (Fawzy et al., 2007; Fawzy, 2008), conventional mineral separation methods is not satisfactory especially at fine sizes. Flotation is the only known available method that can use for separating beryl from quartz in fine sizes. Currently, there is little and old information in the literature about flotation or surface characterization of beryl. The recent paper has been published for studying flotation of beryl is Wang and Yu (2007) that studied the effects of multivalent metallic cations on the flotation behavior of spoumene and beryl.

Magnetic materials are the materials designed to bind selectively on some nonmagnetic materials to make them separable using magnetic separation are called magnetic carriers. A magnetic carrier technology aimed to finding new methods for upgrading and separating of fine and ultra-fine materials.

This technology works as achieving selective adsorption of strongly magnetic phase as magnetite particles on the surface of non-magnetic particles of the desired mineral in the slurry. By adjusting the physicochemical surface properties of the desired mineral and magnetite, magnetite particles selectively attaches to the desired mineral and improves its magnetism. Once the selective attachment takes place, these magnetic parcels can be recovered by magnetic separation (Parsonage, 1988; Qingxia and Friedlaender, 1994; Broomberg et al., 1999; Feng et al., 2000; Anastassakis, 2002). Magnetic carrier technology has been explored both experimentally and theoretically in mineral processing practices. Shubert, 1980 studied the selective separation of non-magnetic minerals such as chalcocite, sphalerite and coal from their associated gangue minerals using magnetic carrier technology. Prakash, et al., 1999, investigated the magnetic separation of calcite using selective coating of synthetic colloidal magnetite with sodium oleate. Ucbas et al., 2014 a&b studied the separation of chromite from serpentine in fine sizes using magnetic carrier technology that used heavy media grade magnetite as carrier. Determination of separation parameters for calcite and apatite using magnetic coating was studied by Tufan et al., 2015. Separation of quartz from magnesite fines using magnetic carrier technology has been studied and investigated that the attachment of fine magnetite onto quartz was possible in the presence of dodecylamine and kerosene in the pH range of 6–11 (Anastassakis, 1999). Lu et al. (2017) discussed the selective surface magnetization technology that employed to separate pentlandite from serpentine by adding fine magnetite coating. Selective recovery of microcrystalline graphite from quartz using hydrophobized magnetite as magnetic seed is studied by Pengfei et al., 2020. These techniques have also found applications in the beneficiation of other minerals, including ferrihydrite, gold, coal, calcite, and dolomite [Parsonage, 1988; Gray et al., 1994; Karapinar, 2003].

Separation of fine beryl from quartz that is considered as the most abundant associated gangue mineral for beryl in its sources is still a big challenging subject with the advances in mineral processing techniques. This study aims to investigate for the first time a possible technique for separating fine beryl from quartz via magnetic carrier technology

2. Materials and methods

2.1. Materials

Pure mineral samples of beryl and quartz were obtained from the dumps of Umm Addebaa in South Eastern Desert of Egypt by crude sieving in the field followed by hand selection. The mineral samples were prepared in the size fractions of $-150+75\ \mu\text{m}$ by crushing and grinding using agate mortar and then dry screening using laboratory sieves, yielding the fractions $-150+75\ \mu\text{m}$ that used for magnetic carrier tests and $-75\ \mu\text{m}$ that used in zeta potential and FTIR measurements. Magnetite was ground for 4 h in mill giving particle size d_{90} of $10\ \mu\text{m}$ to be ready for magnetic carrier tests, zeta potential and FTIR measurements.

Sodium oleate of analytical purity was used to modify the magnetite surface property and obtained from Oxoford laboratory- India, non-ionic surfactant sorbitan monooleate (span 80, 99%) was obtained from LOBA Chemie-India and was used as an adhesion reagent. Analytical grade of sodium hydroxide (99%) and hydrochloric acid (35-37%) were used as pH adjusters and obtained from Alpha Chemicals.

2. Methods

2.2.1. Characterization of samples

Mineralogical confirmation of beryl, quartz and magnetite samples were carried out using X-ray diffraction (XRD) unit Philips PW-3710 with generator PW-1830, Cr target tube and Ni filter at 40 KV and 30 Ma. While the chemical composition and particle size of the mineral samples were checked using scanning electron microscope (SEM). SEM is provided with a Philips XL 30 energy-dispersive spectrometer (EDS) unit

2.2.2. Zeta potential measurements

Malvern zetasizer nano series-zs instrument was used for zeta-potential measurements. For all tests, dilute suspensions were prepared by mixing 0.1 g of mineral powder in $50\ \text{cm}^3$ of 0.01 M NaNO_3

solution as the supporting electrolyte. Sodium hydroxide and hydrochloric acid were used as pH adjuster. All tests were carried out at pH range 2-11, and each experiment was repeated three times to ensure repeatability and provide a standard deviation of the isoelectric point pH value (± 0.1 mV).

2.2.3. Oleate-coated magnetite preparation

Oleate-coated magnetite was prepared by using about 20 g of magnetite and added to 100 mL of 2×10^{-2} M sodium oleate solution, followed by stirring for 20 min. The prepared suspension was then kept still for 24 h to allow sodium oleate to interact with the magnetite surface. Subsequently, the magnetite particles were collected and washed several times with distilled water to remove excessive sodium oleate. Lastly, these magnetite particles were dried at 80°C in an oven.

2.2.4. Magnetic carrier experiments

The experiments were performed in a 100 cm³ beaker. A mechanical stirrer with a plastic impeller was used to keep the particles in the suspension. Initial tests were carried out individually for each mineral (beryl, quartz). 1 gm of mineral was conditioned for 10 min with 75ml of distilled water, 0.5 gm of oleate-coated magnetite was added at the prefixed pH in the absence and presence of 15 ml of 4.29 g/L sorbitan monooleate. After conditioning time, mechanical stirrer was stopped and then free magnetite and magnetite coated particles were removed by using highly magnetic metal rod. Uncoated particles of minerals (beryl or quartz) still in the beaker were weighted after filtering and drying in an oven. The net weight was determined (the weight of uncoated particles subtracted from initial weight) and this value was presented as per cent recovery. The oleate-coated magnetite that adsorbed on the mineral surfaces was removed by ethanol washing for mass balancing purpose. The effects of pH, absence and presence of sorbitan monooleate and percentage of beryl vs oleate-coated magnetite content were studied.

2.2.5. FTIR measurements

The Fourier Transform Infrared (FT-IR) analysis was performed for magnetite, oleate-coated magnetite and sodium oleate for clarifying the adsorption of oleate on the surface of magnetite and forming oleate-coated magnetite. Also, FTIR analyses for pure samples of beryl and quartz were performed before and after treatment with sorbitan monooleate and also sorbitan itself to determine the availability of sorbitan adsorption on the mineral surfaces. JASCO Fourier Transform Infrared 6100 was used for both qualitative and quantitative (for liquid samples) analyses produced by Agilent technologies Company, samples were investigated in spectral range (wave numbers cm⁻¹) from 4000 cm⁻¹ to 400 cm⁻¹ without any treatment.

3. Results and discussion

3.1. Characterization of samples

Pure samples of beryl, quartz and magnetite were mineralogically characterized by using XRD analyses. XRD patterns and values of degree 2θ of characteristic peaks of the pure minerals obtained from X-ray diffraction database can be seen in Fig.1. The diffraction lines are in accordance with reference code no. 0009-0430 for beryl, reference code no. 0005-0490 for quartz and reference code no. 0007-0322 for magnetite. The values of degree 2θ characteristic peaks were quite in accordance with those mineral samples studied that confirming the purity of samples. SEM and EDS analyses were employed to investigate the mineral composition of beryl, quartz and magnetite and also the particle sizes of the samples (Figure 2). It can be seen that magnetite is the finest while beryl is the coarsest mineral. The mineral composition data confirm the purity of the minerals.

3.2. Zeta potential measurements

Zeta potentials are very effective measurements that can be used to characterize the electrical double layer of the mineral surface and can delimitate isoelectric point (IEP) of the mineral surface. IEP is the pH value at which the zeta-potential is zero (Pope and Sutton, 1973). Understanding the zeta-potential

of a minerals, and the IEP, combined with knowledge of a surfactant ionization behavior at various pH levels in aqueous conditions, allows one to predict the mechanism of collector adsorption on the mineral surface (Pope and Sutton, 1973; Cheng et al., 1993; Kosmulski, 2009).

Zeta potential measurements of freshly ground beryl, quartz and magnetite in the absence of sorbitan monooleate as a function of pH are presented in Fig. 3. This figure clearly shows that the isoelectric point (IEP) of beryl and magnetite were determined at pH values of 2.08 and 3.07, respectively, while quartz is negatively charged at all pH values between 2 and 12. The surface charge data of quartz is matched well with the expected trend, having a zeta-potential that is negative across

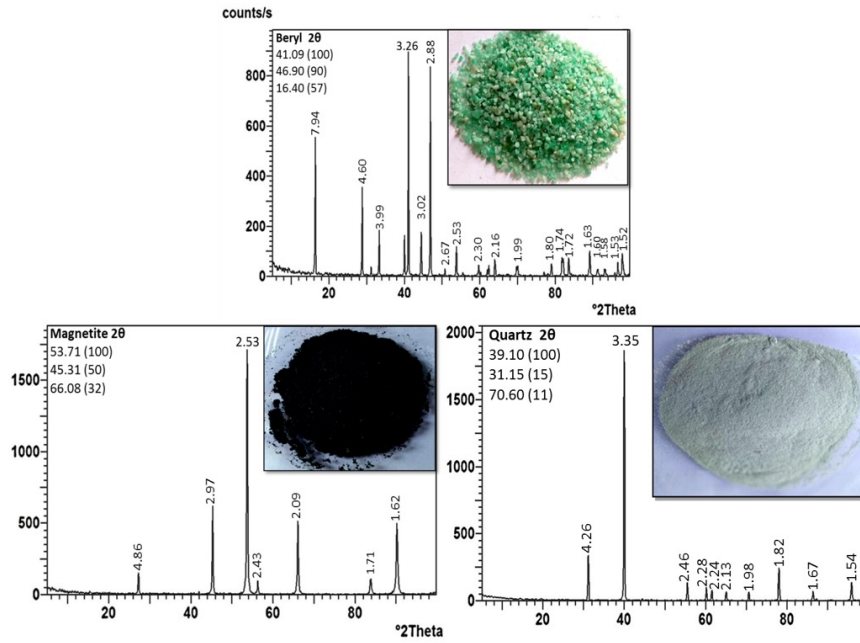


Fig. 1. X-ray diffraction patterns and 2θ characteristic peaks of pure samples of beryl, quartz and magnetite

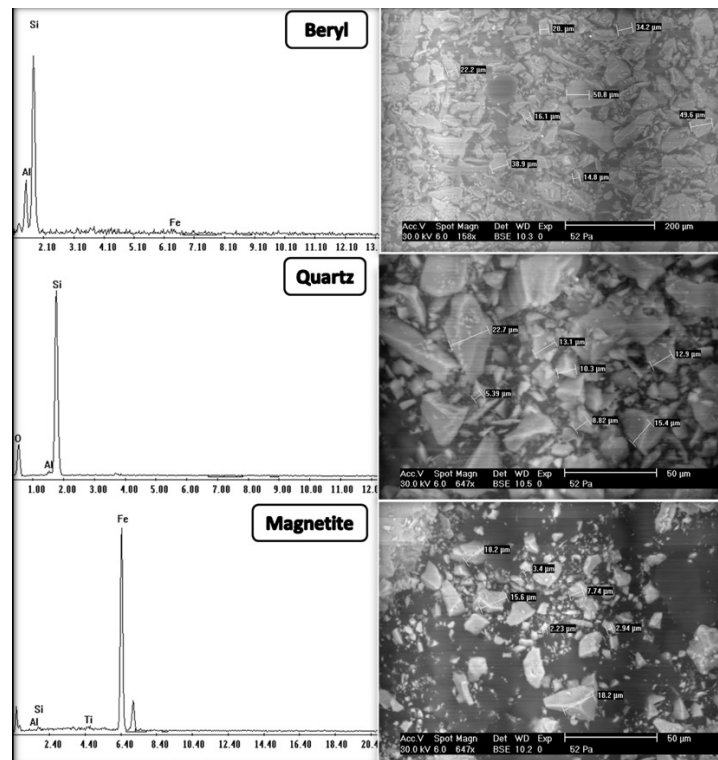


Fig. 2. SEM images and EDS analyses of pure samples of beryl, quartz and magnetite

the pH range investigated, which corresponds to previous work (Kosmulski, 2009). Similar IEP values for beryl were reported in the literature (Toem, 1992 and Yu-hua and Fu-shun, 2007). Some of IEP pH values of magnetite were reported in literature show discrepancies with the data of this work (Broomberg, et al., 1999; Carlson and Kawatra, 2013; Ucbas et al., 2014 b; Pengfei, et al., 2020) while other as Zhang et al., 2020 clarified that IEP of magnetite is around pH 3.0–4.0 that agree with the data of this work.

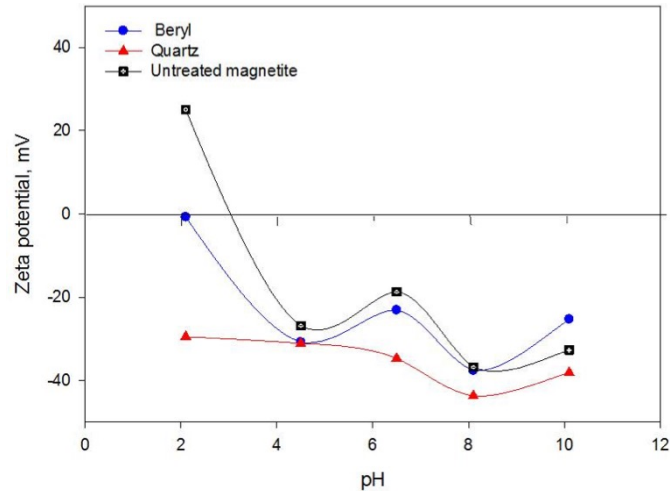


Fig. 3. Zeta potential measurements for beryl, quartz and untreated magnetite as a function of pH

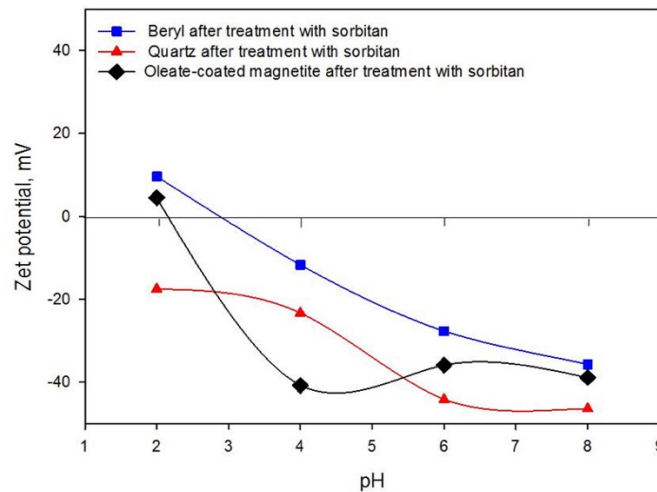


Fig. 4. Zeta potential measurements of beryl, quartz and oleate-coated magnetite after treatment with sorbitan monooleate as a function of pH

3.3. Magnetic carrier tests

Fig. 5 shows the influence of beryl and quartz recovery by pH as well as absence and presence of sorbitan monooleate. It is quite clear that the recovery of beryl decreases with the increase in the pH values as well as the presence of sorbitan monooleate is assisting for increasing beryl recovery. It is shown that the maximum coating of oleate-coated magnetite to the surface of beryl (94% recovery) has taken place at the isoelectric point of beryl (pH 2.08). The adsorption of oleate-coated magnetite on the surface of beryl is affected severely with the presence of non-ionic surfactant (sorbitan monooleate), whereas the beryl recovery reaches of 94% at pH 2.5 with sorbitan while it reaches 44% at the same pH in the absence of sorbitan. Fig. 5 also clarified that quartz recovery slightly effects with change in pH. The adsorption of oleate-coated magnetite on the surface of quartz is weakly affected by the addition of sorbitan monooleate. In order to increase the adsorption of oleate-coated magnetite on the surface of beryl, the effect of increasing the amount of oleate-coated magnetite on beryl recovery were investigated

at pH 2.5 in the presence of sorbitan monooleate and the data shown in Fig. 6. As seen in Fig. 6 beryl recovery could be increased by increasing added oleate-coated magnetite, where beryl recovery increased from 53% to 94% by increasing the amount of oleate-coated magnetite from 0.1 to 0.5 gm.

3.4. FTIR measurements

FTIR measurements were employed for magnetite, sodium oleate and oleate-coated magnetite to elucidate the adsorption of sodium oleate on the surface of magnetite to form oleate-coated magnetite (Fig. 7). According to Stoia et al., 2016, FTIR spectrum of magnetite exhibits two strong infrared adsorption bands at 570 and 390 cm^{-1} . The band at 570 cm^{-1} can be assigned to the Fe-O stretching mode of the tetrahedral and octahedral sites and the band at 390 cm^{-1} can be assigned to the Fe-O stretching mode of the octahedral sites. According to Stoia op. sit., the FTIR spectrum can be considered one of the most appropriate tools for confirming the purity of an iron oxide, or to evidence the presence of a mixture of iron oxides.

Fig. 7 shows that the studied magnetite contains mostly magnetite pure as the band located at 578 cm^{-1} (Fe-O bonding) is sharp and symmetric. The FTIR spectrum also shows water molecule stretching vibration bands at 3435 and 1630 cm^{-1} . The sodium oleate spectra show broad band at 3435.56 cm^{-1} is the characteristics of the O-H stretching vibration of the acid (oleic acid). The band at 2073.1 cm^{-1} is the characteristics for C-C triple bond of alkynes. The strong band at 1636.3 cm^{-1} is the characteristics of C-C double bond. The FTIR bands of magnetite after treatment with 2×10^{-2} sodium oleate are quiet identical to bands observed at wavenumber of 3435.56 cm^{-1} , 1636.3 cm^{-1} and 587 cm^{-1} with the reference spectrum sodium oleate indicating adsorption of sodium oleate on the surface of magnetite forming oleate-coated magnetite.

The infrared spectra of beryl, sorbitan monooleate and beryl after treatment with sorbitan are given in Fig.8. Band at 460 cm^{-1} is Si-O-Si bending vibration while bands at 492 – 522 cm^{-1} are Si-O-Al bending vibration. Si-O and Be-O bond vibration is observed at wavenumber 808 cm^{-1} . Bands at 954 cm^{-1} are characteristics for Si-O vibration of beryl and bands at 1014 cm^{-1} are characterize for internal Si-O stretching vibration while bands at 1171-1203 cm^{-1} are characteristics for Be-O vibration and Si-O stretching vibration (Reshma et al., 2016). Beryl under study was detected with bands at 441.69 cm^{-1} , 495.10 cm^{-1} , 807.48 cm^{-1} , 952.32 cm^{-1} and 1173.26 cm^{-1} . The infrared spectrum of sorbitan monooleate shows that band at 3463.53 cm^{-1} is the characteristic of the O-H stretching vibration of the acid. The strong band at 1637.27 cm^{-1} is the characteristic of C-C double bond. If there is a coupling between C=C group and C=O of ester, the intensity will increase due to the increase in dipole momentum in double bond (Coates, 2000). The infrared spectra of beryl after treatment with 4.29 g/L sorbitan monooleate are completely differ from that before treatment and have quite identical to bands observed at wavenumber of 3463.53 cm^{-1} and 1637.27 cm^{-1} with the reference spectrum of sorbitan monooleate indicating adsorption of sorbitan on the surface of beryl.

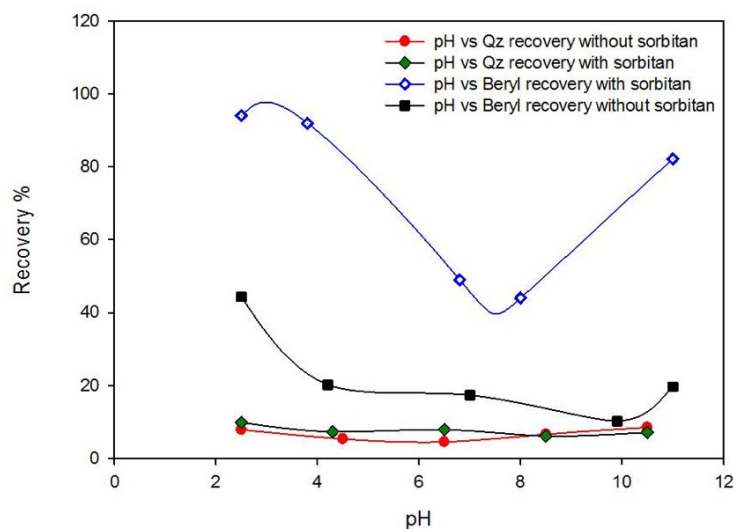


Fig. 5. Effect of pH on beryl and quartz recovery in the presence and absence of sorbitan monooleate

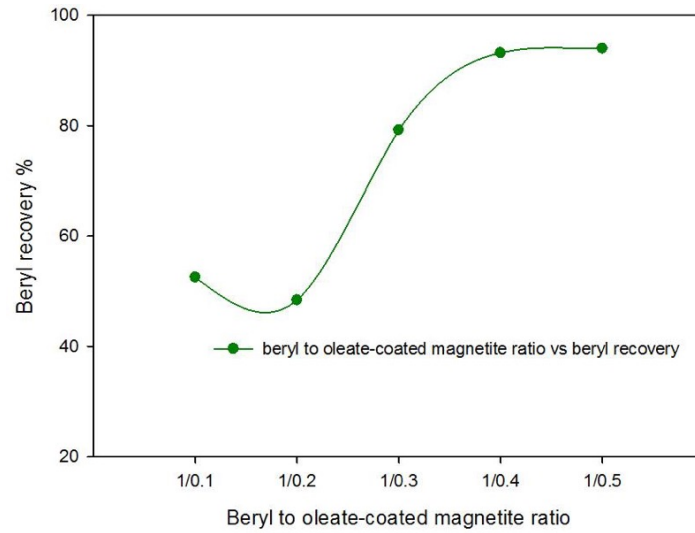


Fig. 6. Effect of beryl to oleate-coated magnetite on beryl recovery

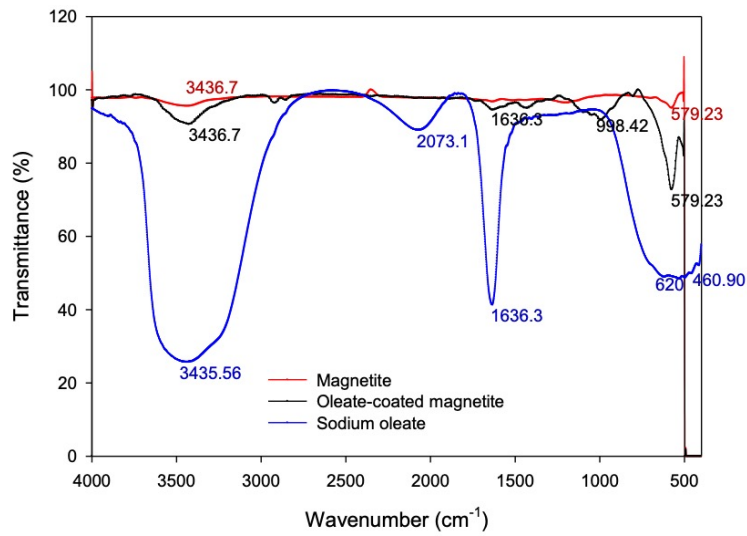


Fig. 7. Infrared spectra of magnetite, oleate-coated magnetite and sodium.

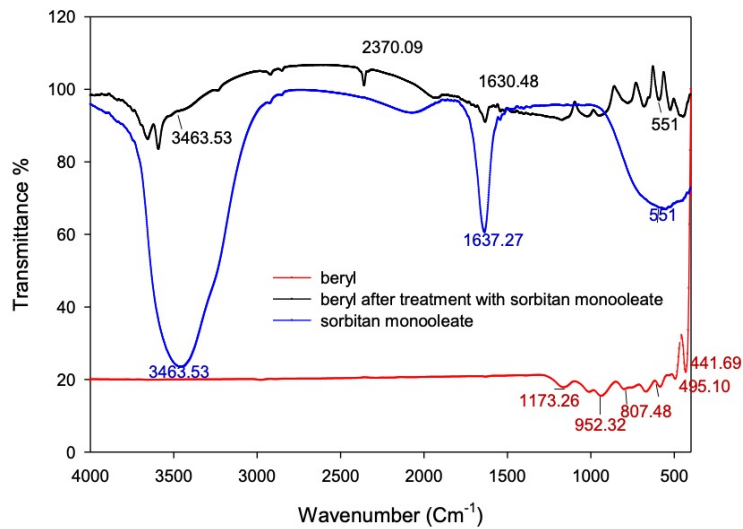


Fig. 8. Infrared spectra of beryl, sorbitan monooleate and beryl after treatment with sorbitan

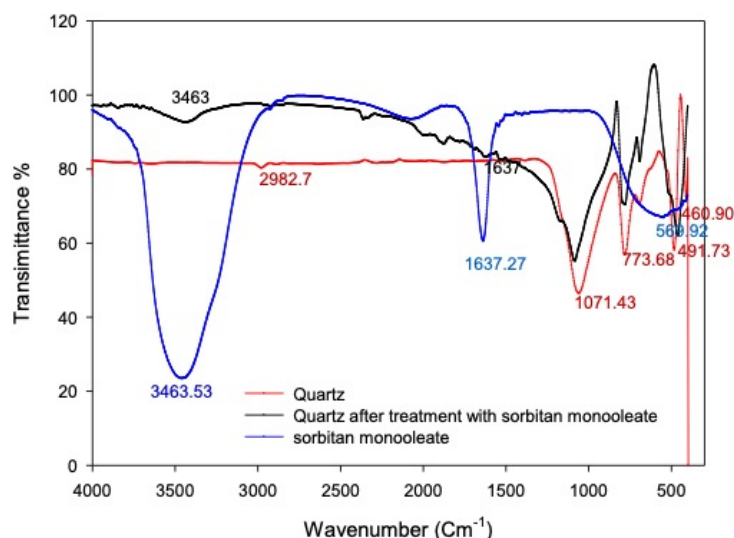


Fig. 9. Infrared spectra of quartz, sorbitan monooleate and quartz after treatment with sorbitan

The infrared spectroscopic analysis of the interaction between quartz and sorbitan monooleate is shown in Fig. 9. The strongest bonds in the silicate structure minerals are Si-O bonds that can be recognized by very strong bands in the region 900 to 1100 cm^{-1} is due to stretching as well as less intense bands in the 400 to 800 cm^{-1} region is due to bending. The studied quartz was detected with bands at 460.90 cm^{-1} , 491.73 cm^{-1} , 773.68 cm^{-1} , and 1071.43 cm^{-1} . In the spectrum of the sorbitan monooleate, there were peaks of the hydroxyl group at 3463.53 cm^{-1} , the strong C=O ester bond at 1637.27 cm^{-1} (Nandiyanto et al., 2019). The infrared spectra of quartz after treatment with 4.29 g/L sorbitan monooleate shows that the intensities of quartz peaks were decreased after treatment with sorbitan as well as absence of the reference spectrum of sorbitan on the surface of quartz that indicates low level of adsorption.

4. Conclusion

Laboratory experiments results on separate minerals of beryl and quartz to determine the factors affecting their separation proved that:

- Zeta potential measurements of freshly ground beryl, quartz and magnetite in the absence of sorbitan monooleate as a function of pH clarified that the isoelectric point (IEP) of beryl and magnetite were determined at pH values of 2.5 and 3.07 respectively while quartz is negatively charged at all pH values between 2 and 12.
- As a result of the magnetic carrier experiments for separating fine beryl from quartz, it is quite clear that the maximum adsorption of oleate-coated magnetite on the surface of beryl takes place at isoelectric point of beryl (pH 2.5) because at this point, the surface of beryl has a net neutral charge and accessible to adsorb magnetite coated with oil with the aiding of sorbitan monooleate that supports this adsorption and strengthens. Whereas at the same pH, the adsorption of oleate-coated magnetite on the surface of quartz appears feeble as the quartz surface is mainly negatively charged and the presence of non-ionic surfactant as sorbitan monooleate couldn't improve anything.
- Zeta potential and FTIR measurements for beryl, quartz and oleate-coated magnetite before and after treating with sorbitan monooleate proved that oleate-coated magnetite physically adsorbed on the beryl surface and could be separated easily from quartz in fine sizes using magnetic carrier technology at beryl IEP of 2.5 pH, 4.29 g/L sorbitan monooleate and 1:0.5 beryl to oleate-coated magnetite ratio, with the aiding of non-ionic surfactant as sorbitan monooleate.

References

ANASTASSAKIS, G.N., 1999. *A Study on the Separation of Magnesite Fines by Magnetic Carrier Methods*, Colloids and Surfaces A: Physicochemical Engineering Aspects, 149, 585-593.

- ANASTASSAKIS, G., 2002. *Separation of fine mineral particles by selective magnetic coating*. J. Colloid and Interface Science. 256, 114-120.
- BROOMBERG, J., GELINAS, S., FINCH, J. XU, Z., 1999. *Review of magnetic carrier technologies for metal ion removal*. Magnetic and Electric Separation. 9, 169-188.
- CARLSON, J.J., KAWATRA, S.K., 2003. *Factors affecting zeta potential of iron oxides*. Mineral Processing & Extractive Metall. Rev., 34, 269-303.
- CHENG, W., HOLTHAM, N., TAM, T., 2000. *Froth Flotation of Monazite and Xenotime*, Miner. Eng., 6, 341-351.
- COATES, J., 2000. *Interpretation of Infrared Spectra, a Practical Approach*, Encyclopedia of Analytical Chemistry, John Wiley & sons Ltd, Chichester, 10815-10837
- FAWZY, M.M., 2008. *Mineralogical and chemical studies on some Egyptian beryl mineralization*. M Sc. Thesis, Helwan Univ., Egypt. 2008.
- FAWZY, M.M., GHARIB M.E., OMAR S.M., ATREES M.S., ABD ELHAI R. EBAID A. R. AND HASSAN M.A., 2007. *Beryl concentration in the mine dumps of the ancient emerald mines of the Eastern Desert, Egypt*, Sedimentological Society of Egypt, vol. 16.
- FENG, D., ALDRICH, C., TAN, H., 2000. *Removal of heavy metal ions by carrier magnetic separation of adsorptive particulates*. Hydrometallurgy, 56, 359-368.
- GRAY, S.R., LANGBERG, D.E., GRAY, N.B., 1994. *Fine mineral recovery with hydrophobic magnetite*. Int. J. Miner. Process., 41, 183-200.
- HARRELL, J.A., 2004. *Archaeological geology of the world's first emerald mine*. Geoscience Canada, 31 (2), 69-76.
- HARRELL, J.A., 2006. *Archaeological geology of Wadi Sikait PalArch's*. J. of Archaeology of Egypt/Egyptology, 4(1), 1-12.
- KARAPINAR, N., 2003. *Magnetic separation of ferrihydrite from wastewater by magnetic seeding and high-gradient magnetic separation*. Int. J. Miner. Process., 71, 45-54.
- KOSMULSKI, M., 2009. *Surface Charging and Points of Zero Charge*, CRC Press, vol. 145, pp. 1092.
- LU, J., YUAN, Z., WANG, N., LU, S., MENG, Q., LIU, J., 2017. *Selective surface magnetization of pentlandite with magnetite and magnetic separation*, Powder Technol., 317, 162-170.
- NANDIYANTO, A., OKTIANI, R., RAGADHITA, R., 2019. *How to read and interpret FTIR spectroscopy of organic material*. Indonesian J. of Science & Technology, 4(1), 79-118.
- PARSONAGE, P., 1988. *Principles of mineral separation by selective magnetic coating*. Int. J. Mineral Processing, 24, 269-293.
- PENGFEI H., LONG L., YAOLI P., HESHENG, Y., GUANGYUAN, X., 2020. *Recovery of microcrystalline graphite from quartz using magnetic seeding*. Minerals, 10, (24), 1-13.
- POPE, I., SUTTON, I., 1973. *The correlation between froth flotation response and collector adsorption from aqueous solution, Part I. titanium dioxide and ferric oxide conditioned in oleate solutions*, Powder Technology, 7, 271-279.
- PRAKASH, S., DAS, B., MOHANTY, J.K., VENUGOPAL, R., 1999. *The recovery of fine iron minerals from quartz and corundum mixtures using selective magnetic coating*. Int. J. Miner. Process., 57, 87-103.
- PRAKASH, S., DAS, B., VENUGOPAL, R., 1999. *Magnetic separation of calcite using selective magnetite coating*, Magnetic and Electrical Separation, 10, 1-19.
- QINGXIA, L., FRIEDLAENDER, F., 1994. *Fine particles processing by magnetic carrier methods*, Minerals Engineering, 7(4), 449-463.
- RESHMA, B., SAKTHIVEL, R., MOHANTY, JK., 2016. *Characterization of low grade natural emerald gemstone*, J. Geology & Geophysics, 6(1), 1-6.
- SHUBERT, R.H., *Magnetic separation of particulate mixtures*, U.S. Patent RE 30.360.1980.
- SINGH, S., SAHOO, H., RATH, S.S., SAHU, A.K., DAS, B., 2015. *Recovery of iron minerals from Indian iron ore slimes using colloidal magnetic coating*. Powder Technol., 269, 38-45.
- STOIA, M., ISTRATIE, R., PACURARIU, C., 2016. *Investigation of magnetite nanoparticles stability in air by thermal analysis and FTIR spectroscopy*. J. Therm. Anal. Calorim., 125, 1185-1198
- TOREM, M.L., PERESI, A.E., ADAMIAN, R., 1992. *On the mechanism of beryl flotation in the presence of some metallic cations*. Minerals Engineering, 5, 1295-1304.
- TUFAN, E., GULER, E., TUFAN, B., COCEN, E., 2015. *Determination of separation parameters for calcite and apatite by magnetic coating*. J. Ore Dressing., 17(34), 1-4.
- UCBAS, Y., BOZKURT, V., BILIR, K., IPEK, H., 2014a. *Separation of chromite from serpentine in fine sizes using magnetic carrier*. Separation Science and Technology, 49, 946-956.

- UCBAS, Y., BOZKURT, V., BILIR, K., IPEK, H., 2014b. *Concentration of chromite by means of magnetic carrier using sodium oleate and other reagents*. Physicochem. Probl. Miner. Process., 50(2), 767-782.
- WANG, Y.-H., YU, F.-S., 2007. *Effects of metallic ions on the flotation of spodumene and beryl*. J. China University of Mining & Technology, 17(1), 35-39.
- ZHANG, J., LIN, S., HAN, M., SU, Q., XIA, L., HUI, Z., 2020. *Adsorption properties of magnetic magnetite nanoparticle for coexistent Cr(VI) and Cu(II) in mixed solution*. Water, 12, 446, 1-13.